Dalton Transactions

ROYAL SOCIETY OF CHEMISTRY

COMMUNICATION

View Article Online
View Journal | View Issue

Cite this: *Dalton Trans.*, 2021, **50**, 12800

Received 20th July 2021,
Accepted 20th August 2021

DOI: 10.1039/d1dt02414k

rsc.li/dalton

Anion recognition by halogen bonding and hydrogen bonding bis(triazole)-imidazolium [2]rotaxanes†

Grace Turner, Andrew Docker and Paul D. Beer *

A novel halogen bonding (XB) bis(iodotriazole)-imidazolium motif is incorporated into the axle component of a [2]rotaxane *via* a discrete chloride anion template directed clipping methodology. ^{1}H NMR anion titration experiments reveal the interlocked host is capable of strong halide and sulfate oxoanion binding in competitive aqueous–organic $CDCl_3/CD_3OD/D_2O$ (45 : 45 : 10 v/v) solvent mixtures. In comparison to a hydrogen bonding rotaxane analogue, which exhibited no pronounced selectivity between Cl^-, I^- and SO_4^{2-}, the axle iodo-triazole donor motifs of the XB rotaxane modulate the anion recognition preference towards the lighter halides $Cl^- \approx Br^- > SO_4^{2-} > I^-$.

Introduction

Negatively charged species are widely pervasive in a plethora of biological, industrial, and environmental spheres.[1] Their importance in a diverse range of fundamental processes has stimulated the development of synthetic host architectures capable of strong and selective anion recognition. To this end, the employment of hydrogen bonding (HB) interactions has been one of the most popular strategies in anion host design.[2–4] In contrast, the considered use of halogen bonding (XB) for the purposes of recognition remains in its infancy.[5–8] Although recent years have realised considerable promise for solution phase XB-mediated recognition, particularly in the context of anion binding, reports remain surprisingly scarce. As a consequence the scope of XB donor motif design and variation is underdeveloped, particularly in combination with arrays of HB donors.[2] Of the commonly employed HB motifs, imidazolium derivatives have featured heavily over the past few decades in anion receptor design, however their continued interest is in no small part due to their ability to bind anions in competitive aqueous media[9] and their proficiency as functional based sensors for challenging bio-molecules.[10–12] In more recent years, iodo-triazoles have emerged as synthetically accessible and highly potent XB donors, and accordingly have received intense interest in the field of anion recognition.[13–28]

Herein we report a novel, potentially synergistic mixed XB/HB anion recognition motif, comprising of a central imidazolium unit with two adjacent iodotriazole groups (Fig. 1). The receptor design exploits a bidentate XB donor array connected *via* flexible methylene linkers to a charge-assisted C—H HB donor. Incorporation of the motif, and its HB analogue, into a stoppered axle component enabled the synthesis of [2]rotaxane host architectures *via* discrete chloride anion templation. ^{1}H NMR anion titration experiments reveal the interlocked architectures are capable of strong halide and oxoanion recognition in highly competitive aqueous–organic solvent mixtures.

Results and discussion

Rotaxane synthesis

The bis-triazole imidazolium containing axle components were prepared according to a multistep synthetic strategy outlined in Scheme 1. *N*-Alkylation of imidazole at the N^1-position with propargyl bromide produced alkyne **1** in 78% yield.[29] A conventional CuAAC reaction with terphenyl stopper azide **2** [30] in the presence of $[Cu(MeCN)_4]PF_6$, DIPEA and the rate acceler-

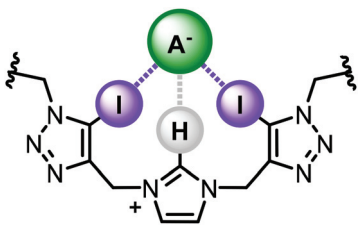

Fig. 1 Target bis-iodotriazole-imidazolium motif and proposed anion binding mode.

Department of Chemistry, University of Oxford, Chemistry Research Laboratory, Mansfield Road, Oxford OX1 3TA, UK. E-mail: paul.beer@chem.ox.ac.uk

†Electronic supplementary information (ESI) available. See DOI: 10.1039/d1dt02414k

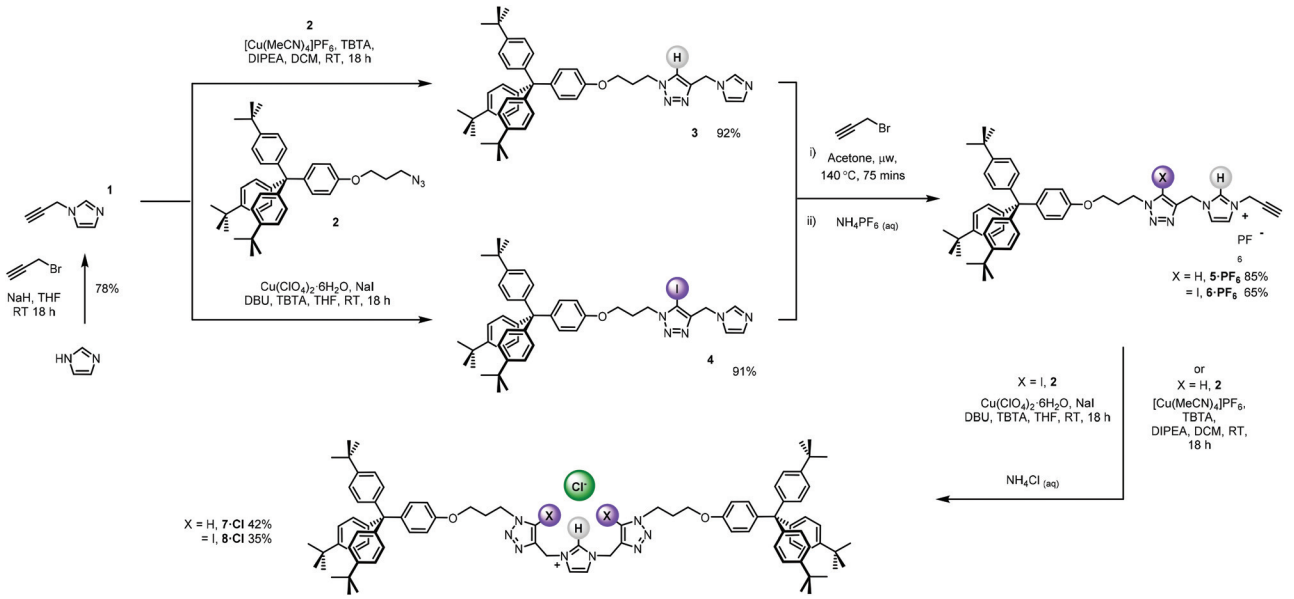

Scheme 1 Synthesis of the bis-iodo/prototriazole imidazolium axle components.

ating ligand TBTA afforded the proto-triazole product **3** in 92% yield. Exploiting the 'one-pot' methodology developed by Zhu *et al.*,[31] treatment of **1** with $Cu(ClO_4)_2{\cdot}H_2O$, NaI and DBU, TBTA and **2** gave the iodo-triazole appended stopper precursor **4** in 93% yield. Installation of the second alkyne group was achieved through a microwave assisted alkylation of the imidazole nitrogen of **3** and **4** with propargyl bromide affording **5·Br** and **6·Br** respectively. Subsequent anion exchange to the non-coordinating hexafluorophosphate salt was achieved through iterative washing of a CH_2Cl_2 solution of the bromide salts with aqueous solutions of NH_4PF_6 to give **5·PF$_6$** and **6·PF$_6$** in 85% and 65% (over two steps) respectively. The alkyne terminated cationic imidazolium axle precursors **5·PF$_6$** and **6·PF$_6$** were subjected to analogous proto- and iodo-triazole copper(I)-catalysed azide alkyne cycloaddition (CuAAC) reaction forming conditions with azide **2**, which after anion exchange gave the desired bis-triazole imidazolium containing axle components as their chloride salts **7·Cl** and **8·Cl** in 42% and 35% yield respectively. The synthesis of the target HB and XB rotaxanes was achieved through a Grubbs'-catalysed chloride anion template ring closing metathesis reaction of **7·Cl** and **8·Cl** with bis-vinyl appended macrocycle precursor **9**[32] in anhydrous dichloromethane over the duration of 4 days (Scheme 2). Purification of the crude reaction mixtures by preparative TLC followed by anion exchange to the non-coordinating hexafluorophosphate salts by copious washing with $NH_4PF_{6(aq)}$ afforded rotaxanes **10·PF$_6$** and **11·PF$_6$** in respective 35% and 24% isolated yields. Both novel rotaxanes were characterised *via* high resolution ESI mass spectrometry and ^{1}H and ^{13}C NMR spectroscopy. Evidence for the successful formation of XB rotaxane **11·PF$_6$** is shown through comparison of ^{1}H NMR spectra of the interlocked product, the macrocycle precursor **9** and axle **8·Cl** (Fig. 2). Upon mechanical bond formation, an upfield shift of imidazolium proton 2 is observed. The signals

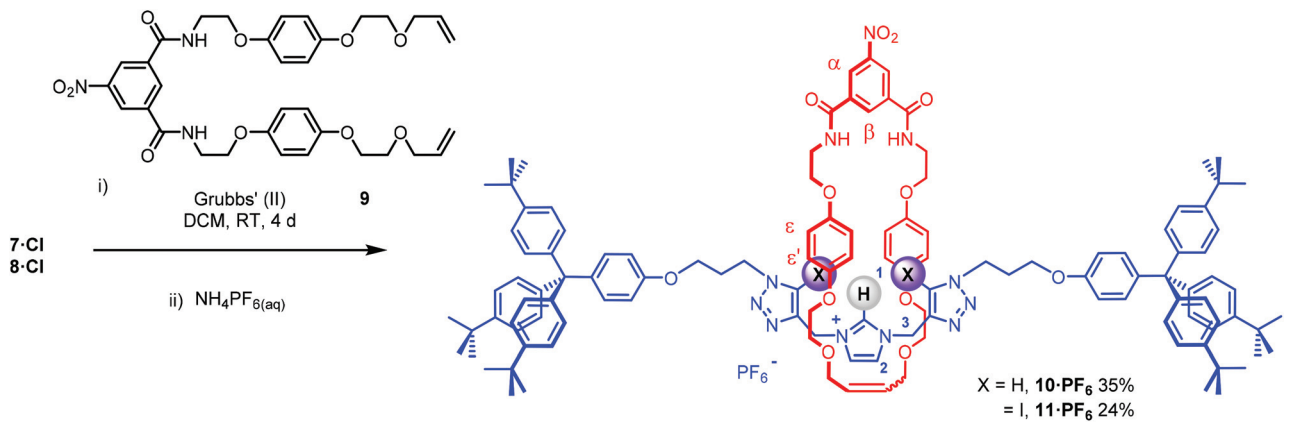

Scheme 2 Chloride anion templated synthesis of the target XB and HB [2]rotaxanes.

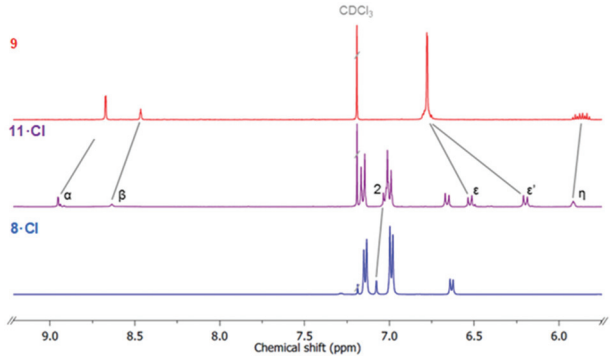

Fig. 2 Stacked truncated ^{1}H NMR spectra of macrocycle precursors **9** (top), XB [2] rotaxane **11·Cl** (middle) and free axle **8·Cl** ($CDCl_3$, 500 MHz, 298 K).

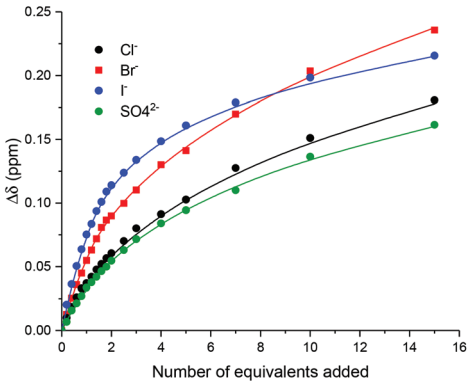

Fig. 3 Experimental titration data (points) and calculated 1 : 2 host : guest stoichiometric binding isotherms (lines) for the addition of anions as their TBA salts to XB rotaxane **11·PF$_6$** monitoring internal macrocycle proton β ($CDCl_3$/CD_3OD/D_2O 45 : 45 : 10, 298 K, 500 MHz).

associated with the macrocycle component hydroquinone environments (ε,ε′) split and move significantly upfield. These diagnostic shifts are due to the favourable donor–acceptor interactions between the electron-deficient imidazolium axle and the electron-rich hydroquinone groups of the macrocycle, indicating the interlocked nature of the product. Substantial downfield shifts of the aromatic protons (α, β) of the macrocycle are also observed. Furthermore, the resonance associated with the terminal alkene protons η confirmed the ring-closing reaction had been successful. Further evidence for the interlocked nature of **11·PF$_6$** was also provided by 2D ROESY NMR spectroscopy (Fig. S1†). Similar chemical shift differences and observations in the 2D ROESY NMR spectrum were observed in the ^{1}H NMR spectrum of HB rotaxane **10·PF$_6$**.

^{1}H NMR anion binding investigations

The anion recognition properties of **10·PF$_6$** and **11·PF$_6$** were investigated by ^{1}H NMR titration experiments in the competitive aqueous–organic solvent mixture $CDCl_3$/CD_3OD/D_2O (45 : 45 : 10 v/v). In a typical experiment the addition of halide or sulfate anion, as their tetrabutylammonium salt, induced significant downfield perturbations in signals associated with the interlocked anion binding cavity, namely internal macrocycle proton β (~0.2–0.3 ppm) and the axle methylene signal 3 (~0.1 ppm). In the case of the HB rotaxane, **10·PF$_6$**, notable downfield shifts of the axle triazole protons were also observed.

Monitoring the shifts of macrocycle proton β, WinEQNMR2 [33] analysis of the titration data (Fig. 3) determined 1 : 2 host : guest stoichiometric association constants, with K_2 values being of much smaller magnitude than K_1 (Table 1). The 1 : 2 host : guest binding stoichiometry may be rationalised by the conformational freedom in the respective rotaxane's axle component by virtue of the methylene linker facilitating, at higher anion equivalents, a second albeit considerably weaker anion binding event, between one iodo- or proto-triazole donor and the C^3 and C^4 protons of the imidazolium group (Fig. 4).

Inspection of Table 1 reveals that both XB and HB rotaxanes exhibited strong halide and sulfate binding in this competitive aqueous–organic solvent mixture. However, it is noteworthy

Table 1 Association constants K_a/M^{-1} for rotaxanes with various anions in $CDCl_3$/CD_3OD/D_2O (45 : 45 : 10 v/v)[a]

	10·PF$_6$		**11·PF$_6$**	
Anion	$K_{1:1}$	$K_{1:2}$	$K_{1:1}$	$K_{1:2}$
Cl^-	2960 (83)	41	3080 (124)	51
Br^-	2110 (73)	77	3200 (132)	41
I^-	2803 (230)	72	2360 (88)	66
SO_4^{2-}	3130 (231)	67	2650 (193)	61

[a] Calculated using WinEQNMR2, estimated standard errors (in parentheses). Anions added as TBA salts. [receptor] = 1 mM, 500 MHz, 298 K.

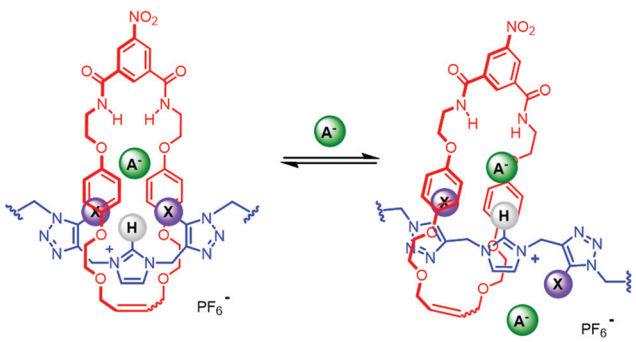

Fig. 4 Postulated 1 : 2 anion binding stoichiometry of the HB and XB [2] rotaxanes **10·PF$_6$** and **11·PF$_6$**.

that the XB rotaxane **11·PF$_6$** displayed an enhanced association constant for bromide over the HB rotaxane analogue **10·PF$_6$**. Furthermore, the XB rotaxane showed a modest preference for the relatively smaller anions (Cl^- = Br^- > SO_4^{2-} > I^-), whereas HB rotaxane displayed no pronounced difference in the K_a values for Cl^-, I^- and SO_4^{2-}. This can be attributed to possible unfavourable steric hindrance effects on the binding of larger anions imparted by the XB rotaxane's axle iodotriazole motifs.

Moreover, it was postulated the imidazolium methylene spacer groups present in the axles of the rotaxanes allow for significant flexibility both within the axle and between the components of the interlocked host, resulting in binding domains capable of accommodating a range of anionic guest species. The flexibility introduced in rotaxanes **10·PF$_6$** and **11·PF$_6$** however, could prove useful for incorporation into [3]rotaxanes, allowing for the binding of larger oxoanions in the binding cavity formed between two macrocycles in a higher order interlocked structure. An attempt to prepare such a [3]rotaxane is discussed in the following section.

Attempted synthesis of hetero[3]rotaxane

The synthesis of a hetero[3]rotaxane using the active metal template (AMT) method[30,34] for mechanical bond formation in combination with the anion template approach was undertaken. Ambitiously, it was envisaged that a chloride-template pseudorotaxane with an axle precursor containing a terminal alkyne, may subsequently be used in an AMT CuAAC 'click' reaction with stopper azide and a suitable copper(I) coordinating macrocycle to produce a hetero[3]rotaxane (Fig. 5).

The capability of stopper precursor imidazolium–alkyne **5·Cl** to participate in anion–template pseudorotaxane assembly formation, as shown in Scheme 3, was investigated initially through a qualitative ^{1}H NMR titration experiment. Stopper imidazolium–alkyne **5·Br** was converted to the chloride salt for the formation of a chloride anion–template pseudorotaxane, by successive washing with $NH_4Cl_{(aq)}$.

The ^{1}H NMR spectrum of an equimolar mixture of isophthalamide macrocycle **12**[35] and **5·Cl** in $CDCl_3$ revealed evidence of successful pseudorotaxane formation *via* the upfield

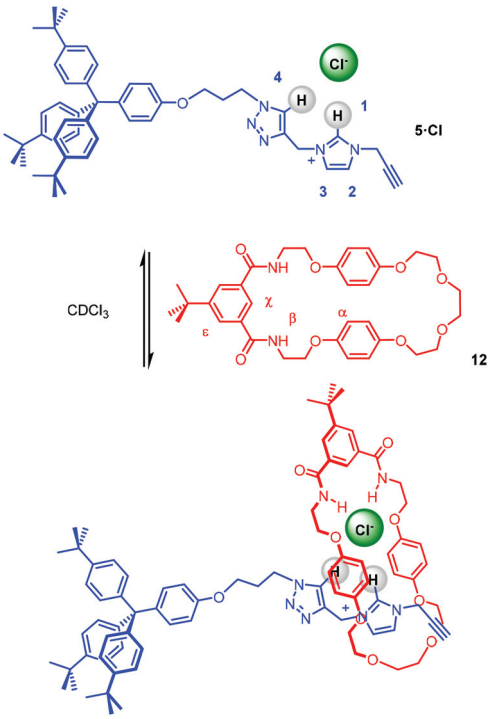

Scheme 3 Pseudorotaxane formation between imidazolium-alkyne thread **5·Cl** and isophthalamide macrocycle **12**.

shifts and splitting of macrocycle hydroquinone protons α and the disappearance of imidazolium proton 1 (Fig. 6). The splitting of the hydroquinone resonances of the macrocycle were due to π–π donor–acceptor interactions between the aromatic systems of the imidazolium-alkyne thread and macrocycle.

After the successful formation of a pseudorotaxane assembly with imidazolium–alkyne **5·Cl** and isophthalamide macrocycle **12**, the synthesis of a hetero[3]rotaxane combining active metal- and anion–template methods was then undertaken (Scheme 4). Five equivalents of stopper imidazolium–alkyne **5·Cl** and macrocycle **12** were initially added to DCM to allow for the formation of the pseudorotaxane. A DCM solution of one equivalent of macrocycle **13**,[36] one equivalent of [Cu(MeCN)$_4$][PF$_6$] and five equivalents of stopper precursor azide

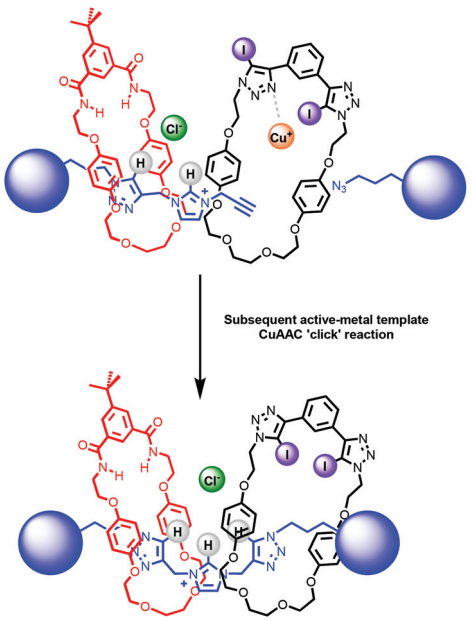

Fig. 5 Schematic representation of route to hetero[3]rotaxane combining chloride anion – template and active–metal template methodologies.

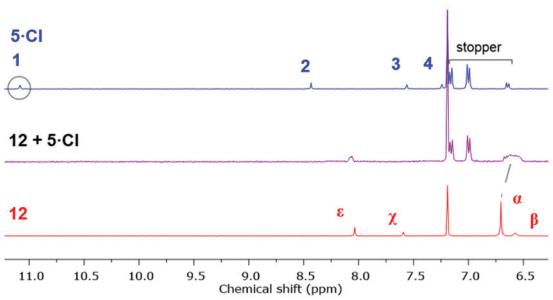

Fig. 6 Truncated ^{1}H NMR spectra (400 mHz, $CDCl_3$, 298 K) of imidazolium-alkyne **5·Cl** (top), an equimolar mixture of macrocycle **12** and **5·Cl** (middle), and macrocycle **12** (bottom).

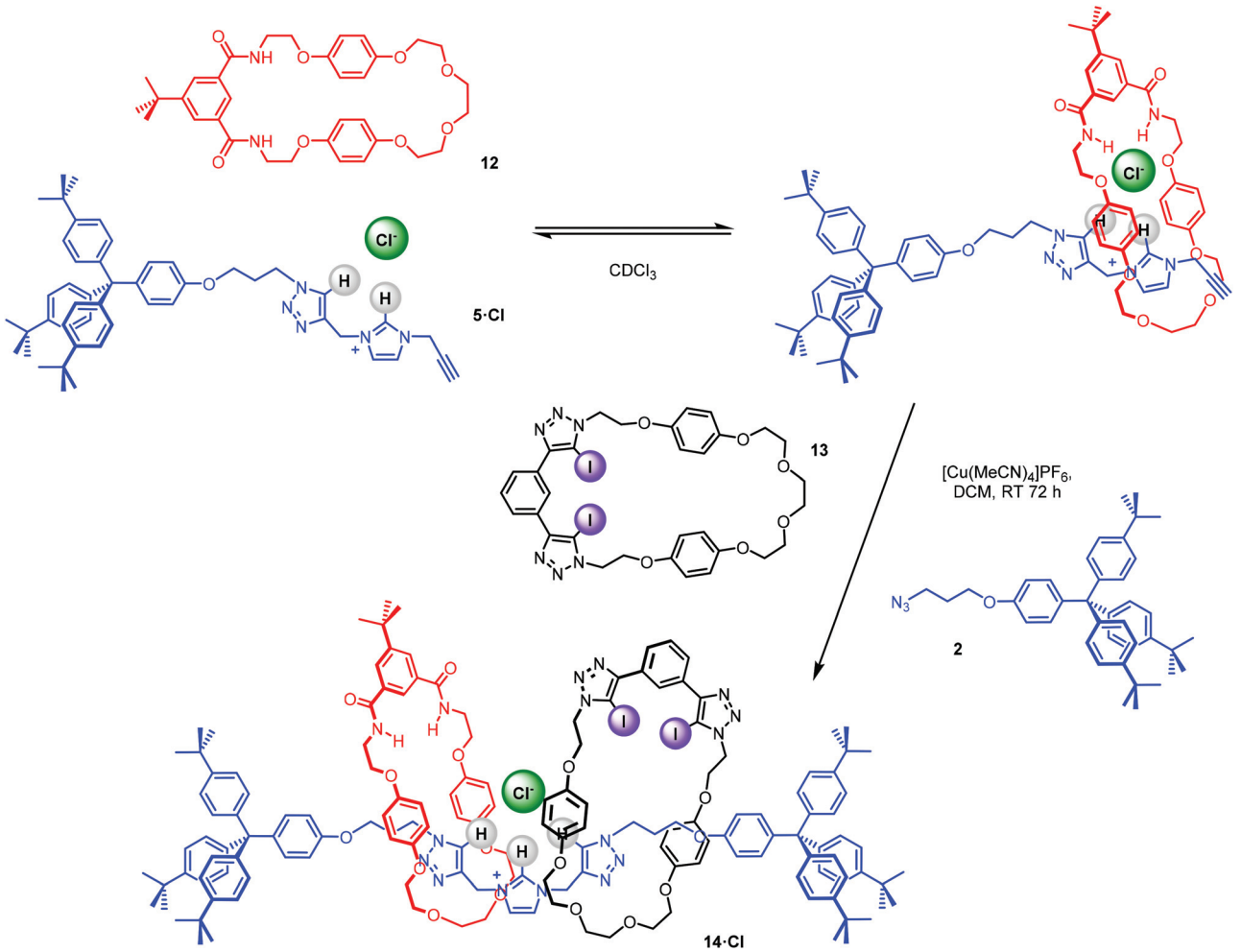

Scheme 4 Attempted synthesis of hetero[3]rotaxane **14·Cl** *via* sequential anion–template pseudorotaxane formation and active–metal template stoppering rotaxanation reaction.

2 was subsequently added and the reaction mixture left to stir for three days. Analysis *via* ESI mass spectroscopy revealed the formation of axle **7** (m/z = 1319.8), a [2]rotaxane containing macrocycle **12** (m/z = 1927.2), a [2]rotaxane with macrocycle **13** (m/z = 2170.9) and most importantly target hetero[3]rotaxane **14·Cl** (m/z = 2778.1) (Fig. 7).

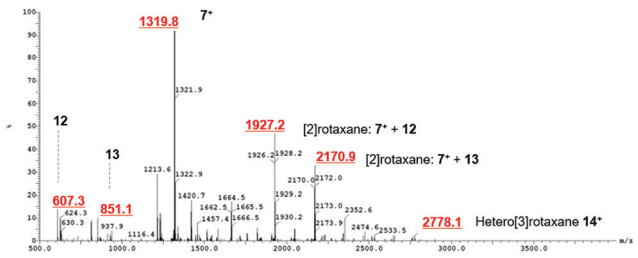

Fig. 7 ESI mass spectrum of crude reaction mixture showing formation of axle 7^+, [2]rotaxane with macrocycle **12**, [2]rotaxane with macrocycle **13** and hetero[3]rotaxane 14^+.

Attempts to isolate the rotaxane products were carried out *via* preparative TLC, using a range of eluents. However, the similar polarities of the interlocked structures negated the successful isolation of the individual rotaxane products. This was nonetheless a promising proof-of-principle result and demonstrated that combining active metal- and anion–template methodologies was a plausible route for the formation of a hetero[3]rotaxane.

Conclusions

In conclusion, new XB and HB [2]rotaxanes incorporating novel bis-iodotriazole- and bis-prototriazole-imidazolium axle motifs were successfully prepared by an anion template methodology. ^{1}H NMR anion titration experiments conducted in $CDCl_3/CD_3OD/D_2O$ (45 : 45 : 10 v/v) reveal both rotaxanes are capable of strong halide and sulfate recognition in competitive aqueous–organic solvent media. In comparison to the HB rotaxane analogue, the anion binding results notably highlight the incorporation of axle iodo-triazole XB donor motifs modu-

late the anion recognition preference for the lighter halides over iodide and sulfate, possibly as a consequence of steric hindrance effects disfavouring the binding of larger anions. An attempt was also made to prepare a novel hetero[3]rotaxane containing the bis-triazole imidazolium donor motif, *via* a combined AMT and chloride-template rotaxanation reaction. Although evidence of the target hetero[3]rotaxane was observed in the ESI mass spectrum of the crude reaction mixture, the higher order rotaxane could not be isolated by chromatographic purification. The integration of XB donor motifs into mechanically bonded interlocked host structural frameworks for aqueous anion recognition applications is continuing in our laboratories.

Conflicts of interest

There are no conflicts to declare.

Acknowledgements

G.T. and A.D thank the EPSRC for studentships (Grant reference numbers EP/M508111/1 and EP/N509711/1).

References

1 M. T. Albelda, J. C. Frías, E. García-España and H.-J. Schneider, *Chem. Soc. Rev.*, 2012, **41**, 3859–3877.
2 P. Molina, F. Zapata and A. Caballero, *Chem. Rev.*, 2017, **117**, 9907–9972.
3 N. Busschaert, C. Caltagirone, W. Van Rossom and P. A. Gale, *Chem. Rev.*, 2015, **115**, 8038–8155.
4 X. Wu, A. M. Gilchrist and P. A. Gale, *Chem*, 2020, **6**, 1296–1309.
5 A. Brown and P. D. Beer, *Chem. Commun.*, 2016, **52**, 8645–8658.
6 L. C. Gilday, S. W. Robinson, T. A. Barendt, M. J. Langton, B. R. Mullaney and P. D. Beer, *Chem. Rev.*, 2015, **115**, 7118–7195.
7 C. J. Massena, N. B. Wageling, D. A. Decato, E. Martin Rodriguez, A. M. Rose and O. B. Berryman, *Angew. Chem., Int. Ed.*, 2016, **55**, 12398–12402.
8 G. Berger, P. Frangville and F. Meyer, *Chem. Commun.*, 2020, **56**, 4970–4981.
9 Z. Xu, S. K. Kim and J. Yoon, *Chem. Soc. Rev.*, 2010, **39**, 1457–1466.
10 H. N. Kim, E.-H. Lee, Z. Xu, H.-E. Kim, H.-S. Lee, J.-H. Lee and J. Yoon, *Biomaterials*, 2012, **33**, 2282–2288.
11 H. N. Kim, J. Lim, H. N. Lee, J.-W. Ryu, M. J. Kim, J. Lee, D.-U. Lee, Y. Kim, S.-J. Kim, K. D. Lee, H.-S. Lee and J. Yoon, *Org. Lett.*, 2011, **13**, 1314–1317.
12 B. Shirinfar, N. Ahmed, Y. S. Park, G.-S. Cho, I. S. Youn, J.-K. Han, H. G. Nam and K. S. Kim, *J. Am. Chem. Soc.*, 2013, **135**, 90–93.
13 F. Ostler, D. G. Piekarski, T. Danelzik, M. S. Taylor and O. G. Mancheño, *Chem. – Eur. J.*, 2021, **27**, 2315–2320.
14 H. A. Klein and P. D. Beer, *Chem. – Eur. J.*, 2019, **25**, 3125–3130.
15 A. Borissov, J. Y. C. Lim, A. Brown, K. E. Christensen, A. L. Thompson, M. D. Smith and P. D. Beer, *Chem. Commun.*, 2017, **53**, 2483–2486.
16 T. Bunchuay, A. Docker, A. J. Martinez-Martinez and P. D. Beer, *Angew. Chem., Int. Ed.*, 2019, **58**, 13823–13827.
17 T. Bunchuay, A. Docker, U. Eiamprasert, P. Surawatanawong, A. Brown and P. D. Beer, *Angew. Chem., Int. Ed.*, 2020, **59**, 12007–12012.
18 R. Tepper, B. Schulze, M. Jäger, C. Friebe, D. H. Scharf, H. Görls and U. S. Schubert, *J. Org. Chem.*, 2015, **80**, 3139–3150.
19 Y. C. Tse, A. Docker, Z. Zhang and P. D. Beer, *Chem. Commun.*, 2021, **57**, 4950–4953.
20 A. Docker, C. H. Guthrie, H. Kuhn and P. D. Beer, *Angew. Chem., Int. Ed.*, 2021, DOI: 10.1002/anie.202108591.
21 A. Docker, T. Bunchuay, M. Ahrens, A. J. Martinez-Martinez and P. D. Beer, *Chem. – Eur. J.*, 2021, **27**, 7837–7841.
22 A. Docker, X. Shang, D. Yuan, H. Kuhn, Z. Zhang, J. J. Davis, P. D. Beer and M. J. Langton, *Angew. Chem., Int. Ed.*, 2021, **60**, 19442–19450.
23 L. E. Bickerton, A. Docker, A. J. Sterling, H. Kuhn, F. Duarte, P. D. Beer and M. J. Langton, *Chem. – Eur. J.*, 2021, **27**, 11738–11745.
24 T. K. Ghosh, S. Mondal, S. Bej, M. Nandi and P. Ghosh, *Dalton Trans.*, 2019, **48**, 4538–4546.
25 J. Pancholi and P. D. Beer, *Coord. Chem. Rev.*, 2020, 213281.
26 R. Tepper, B. Schulze, P. Bellstedt, J. Heidler, H. Görls, M. Jäger and U. S. Schubert, *Chem. Commun.*, 2017, **53**, 2260–2263.
27 S. C. Patrick, R. Hein, A. Docker, P. D. Beer and J. J. Davis, *Chem. – Eur. J.*, 2021, **27**, 10201–10209.
28 A. Docker and P. D. Beer, in *Halog. Bond. Solut*, John Wiley & Sons, Ltd, 2021, pp. 83–120.
29 J. Warnan, Y. Pellegrin, E. Blart and F. Odobel, *Chem. Commun.*, 2011, **48**, 675–677.
30 V. Aucagne, K. D. Hänni, D. A. Leigh, P. J. Lusby and D. B. Walker, *J. Am. Chem. Soc.*, 2006, **128**, 2186–2187.
31 W. S. Brotherton, R. J. Clark and L. Zhu, *J. Org. Chem.*, 2012, **77**, 6443–6455.
32 M. R. Sambrook, P. D. Beer, M. D. Lankshear, R. F. Ludlow and J. A. Wisner, *Org. Biomol. Chem.*, 2006, **4**, 1529–1538.
33 M. J. Hynes, *J. Chem. Soc., Dalton Trans.*, 1993, 311–312.
34 J. D. Crowley, S. M. Goldup, A. L. Lee, D. A. Leigh and R. T. McBurney, *Chem. Soc. Rev.*, 2009, **38**, 1530–1541.
35 M. R. Sambrook, P. D. Beer, J. A. Wisner, R. L. Paul, A. R. Cowley, F. Szemes and M. G. B. Drew, *J. Am. Chem. Soc.*, 2005, **127**, 2292–2302.
36 J. Y. C. Lim, T. Bunchuay and P. D. Beer, *Chem. – Eur. J.*, 2017, **23**, 4700–4707.